AIAA JOURNAL
Vol. 43, No. 8, August 2005

Stiffness Degradation in Hygrothermal Aged Cross-Ply Laminate with Transverse Cracks

A. Tounsi* and K. Amara†
Université de Sidi Bel Abbes, 22000 Sidi Bel Abbes, Algeria

Stiffness degradation resulting from 90-deg ply cracking in hygrothermal aged cross-ply laminates is analyzed. First, the material properties of the composite are affected by the variation of temperature and moisture and are based on a micromechanical model of laminates. Consequently, the hygrothermal conditions degrade the stiffness of the laminate. On the other hand, when this latter is subjected to tensile mechanical loading, the early stage of damage is dominated by matrix cracking in the transverse plies; its presence causes stiffness reduction and can be detrimental to the strength of the laminate. In this investigation, a modified shear-lag analysis, taking into account the hygrothermal effect on the material properties of the laminate, is employed to evaluate the effect of transverse cracks on the stiffness reduction in the hygrothermal aged cross-ply laminated composites. The results represent well the dependence of the degradation of elastic properties on the crack density and hygrothermal conditions.

Nomenclature

E_f	=	Young's modulus of the fiber
E_L	=	longitudinal Young's modulus
E_m	=	Young's modulus of the matrix
E_T	=	transverse Young's modulus
E_x	=	Young's modulus of the damaged laminate
E_{x0}	=	Young's modulus of the undamaged laminate
G_f	=	shear modulus of the fiber
G_{LT}	=	longitudinal shear modulus of ply
G_m	=	shear modulus of the matrix
$G_{\mathrm{TT'}}$	=	transverse shear modulus
h_0	=	ply thickness
l_0	=	half-crack spacing
N_x	=	applied load
R	=	stress perturbation function
S_{ij}	=	compliance matrix of the unidirectional ply
t_0	=	thickness of the 0-deg layer
t_{90}	=	half-thickness of the 90-deg layer
$u_0(x, z)$	=	longitudinal displacement within 0-deg layer
$u_{90}(x, z)$	=	longitudinal displacement within 90-deg layer
V_f	=	fiber volume fraction
V_m	=	matrix volume fraction
ζ	=	shear-lag parameter
ν_f	=	Poisson's ratio of the fiber
ν_{LT}	=	Poisson's ratio
ν_m	=	Poisson's ratio of the matrix
ρ	=	crack density
σ_c	=	applied stress

I. Introduction

MATRIX cracking has long been recognized as the first damage mode observed in composite laminates under static and fatigue tensile loading. It does not necessarily result in the immediate catastrophic failure of the laminate and therefore can be tolerated. However, its presence causes stiffness reduction and can be detrimental to the strength of the laminate. Many analyses have been developed which attempt to evaluate the stiffness loss in the cracked laminate. The shear-lag method[1−9] and variational methods[10−12] are among the most commonly used procedures. Stiffness reduction caused by the transverse matrix cracks in various composite laminates has been studied by Highsmith and Reifsnider[1] using the shear-lag method. They assumed a thin boundary layer, referred to as a shear layer, in the vicinity of the layer interface. Tensile stresses in the uncracked layers are transferred to the cracked layers via the shear layer. They also assumed that shear stresses are not dominant within the boundary layer. The procedure for finding the stiffness reduction is simple. However, it is not easy to determine the thickness of the boundary layer.

Flaggs[2] studied tensile matrix failure in composites laminates. The analysis was based on the two-dimensional shear-lag theory with the use of mixed-mode strain-energy release rate. Even though good agreement was observed with experimental data for thinner 90-deg layers, this analysis is not applicable for thicker 90-deg layers.

Laws and Dvorak[3] practised the shear-lag concept to deduce the degraded stiffnesses of a cracked cross-ply laminate taking the effects of residual stresses into consideration. It was pointed out that residual stresses give rise to permanent strains when the applied load is large enough to cause transverse cracking, and further that these strains actually are negligible.

Lim and Hong[4,5] applied the shear-lag model to a cross-ply laminate and also included the effects of thermal residual stresses. It was established that the thermal residual stresses significantly influence the transverse cracking in graphite/epoxy laminates, more so than in glass/epoxy composite systems. This is discernible because the graphite/epoxy systems have a higher degree of orthotropy in elastic constants as well as in thermal expansion coefficients.

Lee and Daniel[6] proposed a simplified shear-lag analysis that used a progressive damage scheme. It was assumed that the next set of cracks was developed when the maximum axial stress in the plies reached the strength of the layer. They assumed linear shear-stress distributions in each layer throughout the thickness. In their formulation, a shear-stress-free condition on the crack surface is not satisfied. Berthelot et al.,[7] Berthelot,[8] and Berthelot and Le Corre[9] employed a shear-lag concept to obtain the general form of the stress distributions in 0- and 90-deg layers. They proposed a particular form of the variation of the longitudinal displacement across the thickness of 0-deg plies, which yields a good agreement of the stress distributions with finite element analysis. Stiffness reduction in a transversely cracked cross-ply fiber composite laminate was studied by Hashin[10] using variational method. The normal-ply

Received 16 July 2003; revision received 7 February 2005; accepted for publication 20 February 2005.

*Associate Professor, Laboratoire des Matériaux et Hydrologie, B.P. 89, Cité Ben M'hidi; tou_abdel@yahoo.fr.

†Ph.D. Student, Laboratoire des Matériaux et Hydrologie, B.P. 89, Cité Ben M'hidi.

stress in the load direction was assumed to be constant over the ply thickness. The stiffness reduction caused by transverse cracking is in good agreement with the experimental results. However, damage progression and accumulation cannot be determined by using this analysis. The principle of minimum complementary energy was also used by Varna and Berglund[11] to predict the stress fields in a cracked cross-ply laminate. The strain-energy release rate has also been calculated by Nairn[12] using a variational analysis. It is a two-dimensional thermoelastic analysis assuming that normal-ply stress in the load direction to be constant over the ply thickness. Dharani and Tang[13] have described a consistent shear-lag theory analysis for both microcracking and microcrack induced delaminations. They predicted failure using numerical stress calculations and a point-stress failure criterion. Many of their predictions are in qualitative agreement with experimental results. Selvarathinam and Weitsman[14] have employed the finite element method to model the competition between the transverse cracking and delamination modes of failure that occur in cross-ply AS4/3501-6 gr/ep coupons subjected to fatigue.

The present study extends the previous works to the case of aged cross-ply laminates. It is well known that during the operational life the variation of temperature and moisture reduces the elastic moduli and degrades the strength of the laminated material.[15–19] In the present paper, both ambient temperature and moisture are assumed to have a uniform distribution. The plate is fully saturated such that the variation of temperature and moisture are independent of time and position. Complete parabolic shear-lag analysis and progressive shear model[8,9] are used with some modifications to predict the effect of transverse cracks on the stiffness degradation of aged composite laminates. First, the general expression for longitudinal modulus reduction vs transverse crack density is obtained by introducing the stress perturbation function. Good agreement is obtained comparing prediction with experimental results and Hashin's model. This latter is also modified by introducing the stress perturbation function. In the second part of this investigation, the hygrothermal effect on the material properties of the laminate is taken into account to evaluate the relative and the total stiffness loss in cross-ply laminates containing transverse cracks. In this study, the hygrothermal stresses[20–25] and the water-induced microcracks[26] are not taken into consideration. The obtained results illustrate well the dependence of the degradation of elastic properties on the crack density and hygrothermal conditions.

II. Theoretical Modeling

It is well known in many studies[15–19] that the material properties are functions of temperature and moisture. In terms of a micromechanical model of laminate, the material properties can be written as[27]

$$E_L = V_f E_f + V_m E_m \tag{1}$$

$$\frac{1}{E_T} = \frac{V_f}{E_f} + \frac{V_m}{E_m} - V_f V_m \frac{\nu_f^2 (E_m/E_f) + \nu_m^2 (E_f/E_m) - 2\nu_f \nu_m}{V_f E_f + V_m E_m} \tag{2}$$

$$\frac{1}{G_{\mathrm{LT}}} = \frac{V_f}{G_f} + \frac{V_m}{G_m} \tag{3}$$

$$\nu_{\mathrm{LT}} = V_f \nu_f + V_m \nu_m \tag{4}$$

In the preceding equations, V_f and V_m are related by

$$V_f + V_m = 1 \tag{5}$$

It is assumed that E_m is a function of temperature and moisture, as is shown in Sec. III.B, then E_L, E_T, and G_{LT} are also functions of temperature and moisture.

A. Model Formulation

In the present analysis, we have modified the two models[7–9] (complete parabolic shear-lag model and progressive shear-lag model) by using the same methodology developed by Joffe et al.[28] to study the transverse cracking problem in $[\mathrm{S}/90_n]_S$ laminates.

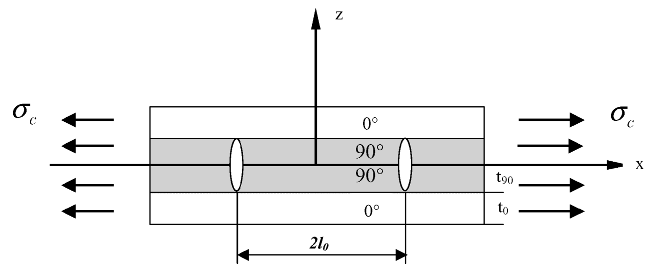

Fig. 1 Transverse cracked cross-ply laminate and geometric model.

Consider the idealized cross-ply laminates shown in Fig. 1. When such laminate is loaded in uniaxial tension, the first damage that occurs is transverse cracking in the middle layer. The spacing between cracks is assumed to be equidistant, which means that laminate contains a periodical array of cracks in 90-deg layer. The geometry of the repeatable unit used for modeling is shown in Fig. 1. Dimensionless coordinates can be introduced:

$$\bar{z} = z/t_{90}, \qquad \bar{l}_0 = l_0/t_{90}, \qquad \alpha = t_0/t_{90}$$
$$\bar{x} = x/t_{90}, \qquad h = t_0 + t_{90} \tag{6}$$

Loading is applied only in x direction, and the far-field applied stress is defined by $\sigma_C = (1/2h)N_x$.

The following analysis will be performed assuming the generalized plane-strain condition:

$$\varepsilon_y^0 = \varepsilon_y^{90} = \varepsilon_y = \text{const} \tag{7}$$

The symbol – over stress and strain components denotes volume average. They are calculated by using the following expressions:

1) In the 0-deg layer,

$$\bar{f}^0 = \frac{1}{2l_0}\frac{1}{t_0}\int_{-l_0}^{+l_0}\int_{t_{90}}^{h} f^0 \,\mathrm{d}x\,\mathrm{d}z = \frac{1}{2\bar{l}_0}\frac{1}{\alpha}\int_{-\bar{l}_0}^{+\bar{l}_0}\int_{1}^{\bar{h}} f^0(\bar{x},\bar{z})\,\mathrm{d}\bar{x}\,\mathrm{d}\bar{z} \tag{8}$$

2) In the 90-deg layer,

$$\bar{f}^{90} = \frac{1}{2l_0}\frac{1}{t_{90}}\int_{-l_0}^{+l_0}\int_{0}^{t_{90}} f^{90}\,\mathrm{d}x\,\mathrm{d}z = \frac{1}{2\bar{l}_0}\int_{-\bar{l}_0}^{+\bar{l}_0}\int_{0}^{1} f^{90}(\bar{x},\bar{z})\,\mathrm{d}\bar{x}\,\mathrm{d}\bar{z} \tag{9}$$

By using the strains in the 0-deg layer (which is not damaged and, hence, strains are equal to laminate strains, $\varepsilon_x = \bar{\varepsilon}_x^0$, etc.) and assuming that the residual stresses are zero ($\Delta T = 0$), the Young's modulus of the laminate with cracks can be defined from following expression:

$$E_x = \sigma_c \big/ \bar{\varepsilon}_x^0 \tag{10}$$

Note that the initial laminate modulus measured at the same load is $E_{x0} = \sigma_c/\varepsilon_{x0}$, and, hence,

$$E_x/E_{x0} = \varepsilon_{x0} \big/ \bar{\varepsilon}_x^0 \tag{11}$$

B. Averaged Stress-Strain Relationships for Laminates with Cracks

Constitutive equations that give the relationship between strain and stresses are as follows:

1) In the 90-deg layer,

$$\begin{Bmatrix} \varepsilon_x^{90} \\ \varepsilon_y^{90} \\ \varepsilon_z^{90} \end{Bmatrix} = \begin{bmatrix} S_{yy} & S_{xy} & S_{yz} \\ S_{xy} & S_{xx} & S_{xy} \\ S_{yz} & S_{xy} & S_{yy} \end{bmatrix} \begin{Bmatrix} \sigma_x^{90} \\ \sigma_y^{90} \\ \sigma_z^{90} \end{Bmatrix} \tag{12}$$

2) In the sublaminate 0 deg,

$$\begin{Bmatrix}\varepsilon_x^0\\ \varepsilon_y^0\\ \varepsilon_z^0\end{Bmatrix} = \begin{bmatrix}S_{xx} & S_{xy} & S_{xz}\\ S_{xy} & S_{yy} & S_{yz}\\ S_{xz} & S_{yz} & S_{zz}\end{bmatrix}\begin{Bmatrix}\sigma_x^0\\ \sigma_y^0\\ \sigma_z^0\end{Bmatrix} \tag{13}$$

where S_{ij} is the compliance matrix for unidirectional composite with 0-deg fiber orientation. To calculate the laminate elastic property, we need $\bar{\varepsilon}_x^0$. By averaging Eqs. (12) and (13), we obtain averaged constitutive equations of the 90- and 0-deg layers. In averaged relationships we have $\bar{\sigma}_z^{90} = \bar{\sigma}_z^0 = 0$, which follows from the force equilibrium in the z direction:

$$\int_{-l_0}^{+l_0} \sigma_z^i \, \mathrm{d}x = 0 \qquad i = 90, 0 \tag{14}$$

Averaged constitutive equations corresponding to in-plane normal stress and strain components are

$$\begin{Bmatrix}\bar{\varepsilon}_x^0\\ \varepsilon_y\end{Bmatrix} = \begin{bmatrix}S_{xx} & S_{xy}\\ S_{xy} & S_{yy}\end{bmatrix}\begin{Bmatrix}\bar{\sigma}_x^0\\ \bar{\sigma}_y^0\end{Bmatrix} \tag{15}$$

$$\begin{Bmatrix}\bar{\varepsilon}_x^{90}\\ \varepsilon_y\end{Bmatrix} = \begin{bmatrix}S_{yy} & S_{xy}\\ S_{xy} & S_{xx}\end{bmatrix}\begin{Bmatrix}\bar{\sigma}_x^{90}\\ \bar{\sigma}_y^{90}\end{Bmatrix} \tag{16}$$

Equations (15) and (16) are obtained from the three-dimensional strain-stress relationships, but because of Eq. (14) the result is similar as in classical thin-laminate theory (CLT). In fact, for an undamaged laminate the averaged stresses and strains are equal to the laminate theory stresses, and strains and Eqs. (15) and (16) are still applicable.

The force equilibrium equations for a damaged (or undamaged) laminate are as follows:

1) In the x direction,

$$N_x = \int_0^{t_{90}} \sigma_x^{90} \, \mathrm{d}z + \int_{t_{90}}^{h} \sigma_x^0 \, \mathrm{d}z = \sigma_c(t_{90} + t_0) \tag{17}$$

leading to

$$\bar{\sigma}_x^{90} t_{90} + \bar{\sigma}_x^0 t_0 = \sigma_c(t_{90} + t_0) \tag{18}$$

2) In the y direction,

$$N_y = 0 \Rightarrow \int_0^{t_{90}} \sigma_y^{90} \, \mathrm{d}z + \int_{t_{90}}^{h} \sigma_y^0 \, \mathrm{d}z = 0 \tag{19}$$

from which follows

$$\bar{\sigma}_y^{90} t_{90} + \bar{\sigma}_y^0 t_0 = 0 \tag{20}$$

Equations (15), (16), (18), and (20) contain seven unknowns: four stress components and three strain components ($\bar{\varepsilon}_x^{90}$, $\bar{\varepsilon}_x^0$, and ε_y). The total number of equations is six. Hence, one of the unknowns can be considered as independent, and the rest of them can be expressed as linear functions of it. Choosing the stress $\bar{\sigma}_x^{90}$ as independent and solving with respect to it the system of Eqs. (15), (16), (18), and (20), we obtain

$$\varepsilon_y = g_1\bar{\sigma}_x^{90} + f_1\sigma_c, \qquad \bar{\varepsilon}_x^{90} = g_2\bar{\sigma}_x^{90} + f_2\sigma_c$$

$$\bar{\varepsilon}_x^0 = g_3\bar{\sigma}_x^{90} + f_3\sigma_c \tag{21}$$

Expressions for g_i, f_i, $i = 1, 2, 3$ through laminate geometry and properties of constituents are given as follows:

$$g_1 = t_{90}\frac{S_{xy}S_{yy} - S_{xx}S_{xy}}{S_{xx}t_0 + S_{yy}t_{90}}, \qquad f_1 = \frac{S_{xx}S_{xy}(t_0 + t_{90})}{S_{xx}t_0 + S_{yy}t_{90}} \tag{22}$$

$$g_2 = S_{yy} - \frac{S_{xy}^2(t_0 + t_{90})}{S_{xx}t_0 + S_{yy}t_{90}}, \qquad f_2 = \frac{S_{xy}^2(t_0 + t_{90})}{S_{xx}t_0 + S_{yy}t_{90}} \tag{23}$$

$$g_3 = \frac{t_{90}}{t_0}\left[\frac{S_{xy}^2(t_0 + t_{90})}{S_{xx}t_0 + S_{yy}t_{90}} - S_{xx}\right]$$

$$f_3 = \frac{t_0 + t_{90}}{t_0}\left(S_{xx} - \frac{S_{xy}^2 t_{90}}{S_{xx}t_0 + S_{yy}t_{90}}\right) \tag{24}$$

C. Stress and Strain Perturbation Caused by Cracks

To obtain an expression for average stress $\bar{\sigma}_x^{90}$ in the repeatable unit, we consider the axial-stress perturbation caused by the presence of two cracks. Without losing generality the axial-stress distribution can be written in the following form:

$$\sigma_x^{90} = \sigma_{x0}^{90} - \sigma_{x0}^{90} f_1(\bar{x}, \bar{z}) \tag{25}$$

$$\sigma_x^0 = \sigma_{x0}^0 + \sigma_{x0}^{90} f_2(\bar{x}, \bar{z}) \tag{26}$$

where σ_{x0}^{90} is the CLT stress in the 90-deg layer, σ_{x0}^0 is the CLT stress in the 0-deg layer (laminate theory routine), and $-\sigma_{x0}^{90} f_1(\bar{x}, \bar{z})$ and $\sigma_{x0}^{90} f_2(\bar{x}, \bar{z})$ are stress perturbation caused by the presence of crack. Normalizing factors in form of far-field stresses in perturbation functions are used for convenience. Averaging Eqs. (25) and (26) and using the integral force equilibrium in the x direction equation (17), we obtain

$$\bar{\sigma}_x^{90} = \sigma_{x0}^{90} - \sigma_{x0}^{90}(1/2\bar{l}_0)R(\bar{l}_0) \tag{27}$$

$$\bar{\sigma}_x^0 = \sigma_{x0}^0 + \sigma_{x0}^{90}(1/2\bar{l}_0\bar{t}_0)R(\bar{l}_0) \tag{28}$$

The function

$$R(\bar{l}_0) = \int_{-\bar{l}_0}^{+\bar{l}_0}\int_0^1 f_1(\bar{x}, \bar{z}) \, \mathrm{d}\bar{z} \, \mathrm{d}\bar{x} \tag{29}$$

is called the stress perturbation function. It is related to axial-stress perturbation in the 90-deg layer and depends on crack spacing (crack density).

The average stress $\bar{\sigma}_x^{90}$ involved in Eq. (21) is now expressed through the stress perturbation function Eq. (29). Conditions used to obtain expressions Eq. (21) are the same as used in CLT. Hence, substituting $\bar{\sigma}_x^{90} = \sigma_{x0}^{90}$, where σ_{x0}^{90} is the x axis stress in the 90-deg layer according to CLT, we obtain CLT solution: $\bar{\varepsilon}_x^{90} = \varepsilon_{x0}^{90} = \varepsilon_{x0}$, $\bar{\varepsilon}_x^0 = \varepsilon_{x0}^0 = \varepsilon_{x0}$, and $\varepsilon_y = \varepsilon_{y0}$.

Substituting Eq. (27), which contains two terms, in Eq. (21), the result has two terms. The first term according to the preceding discussion is equal to CLT strain, but the second one is a new term related to the stress perturbation function $R(\bar{l}_0)$:

$$\varepsilon_y = \varepsilon_{y0} - \sigma_{x0}^{90} g_1(1/2\bar{l}_0)R(\bar{l}_0) \tag{30}$$

$$\bar{\varepsilon}_x^{90} = \varepsilon_{x0} - \sigma_{x0}^{90} g_2(1/2\bar{l}_0)R(\bar{l}_0) \tag{31}$$

$$\bar{\varepsilon}_x^0 = \varepsilon_{x0} - \sigma_{x0}^{90} g_3(1/2\bar{l}_0)R(\bar{l}_0) \tag{32}$$

The stress σ_{x0}^{90} in the 90-deg layer of an undamaged laminate under mechanical loading can be calculated by using CLT:

$$\sigma_{x0}^{90} = Q_{yy}\varepsilon_{x0}\left(1 - \nu_{xy}\nu_{xy}^0\right) \tag{33}$$

Here, ν_{xy}^0 is the Poisson's ration of the undamaged laminate.

D. Expressions for Longitudinal Young's Modulus Reduction

To derive the expression for the longitudinal modulus E_x of the damaged laminate, we use definitions Eq. (10) and substitute Eqs. (30) and (32) in these relationships. Finally we use Eq. (33). This procedure yields

$$E_x/E_{x0} = 1/[1 + a\bar{\rho}R(\bar{l}_0)] \tag{34}$$

where $\bar{\rho} = 1/2\bar{l}_0$ is normalized crack density and a is known function, dependent on the elastic properties and geometry of the 0- and 90-deg layers:

$$a = \frac{E_{90}t_{90}}{E_0 t_0}\left(\frac{1-\nu_{xy}\nu_{xy}^0}{1-\nu_{xy}\nu_{yx}}\right)\left[1+\frac{\nu_{xy}S_{xy}(t_0+t_{90})}{S_{xx}t_0+S_{yy}t_{90}}\right] \tag{35}$$

E_0 and E_{90} are the Young's moduli of the 0- and 90-deg layers, respectively.

From Eqs. (34) and (35) it is clear that the function $R(\bar{l}_0)$ is the only unknown. Hence, reduction of the longitudinal modulus depends on the form of this function of crack spacing (density). The solution for this function can be found by using different analytical models such as shear-lag models or variational models (for example, Hashin's model).

E. Computation of the Stress Perturbation Function

1. Shear Lag Model

This is the simplest stress-transfer model. There are a number of modifications for this model. Here, we have used two models developed by Berthelot et al.,[7] Berthelot,[8] and Berthelot and Le Corre.[9] These latter are modified by introducing the stress perturbation function. It can be shown that the stress perturbation function $R(\bar{l}_0)$ is found in the following form:

$$R(\bar{l}_0) = \int_{-\bar{l}_0}^{+\bar{l}_0}\frac{\cosh(\xi\bar{x})}{\cosh(\xi\bar{l}_0)}\,\mathrm{d}\bar{x} = \frac{2}{\xi}\tanh(\xi\bar{l}_0) \tag{36}$$

where ξ is the shear-lag parameter

$$\xi^2 = \bar{G}\frac{t_{90}(t_{90}E_{90}+t_0E_0)}{t_0E_0E_{90}} \tag{37}$$

The coefficient $\bar{G}$ depends on used assumptions about the longitudinal displacements and shear-stress distribution:

1) For assumptions on the longitudinal displacements, the variation of the longitudinal displacement is supposed to be parabolic in the thickness of the 90-deg layer,

$$u_{90}(x,z) = \bar{u}_{90}(x) + \left[z^2 - \left(t_{90}^2/3\right)\right]A_{90}(x) \tag{38}$$

the variation of the longitudinal displacement is to be determined in the thickness of the 0-deg layers,

$$u_0(x,z) = \bar{u}_0(x) + f(z)A_0(x) \tag{39}$$

2) For assumptions on the shear stresses, similar in 0- and 90-deg layers, which can be obtained by assuming that the transverse displacement is independent of the longitudinal coordinate:

$$\sigma_{xz}^i = G_{xz}^i\gamma_{xz}^i, \qquad \gamma_{xz}^i = \frac{\partial u_i}{\partial z} + \frac{\partial w_i}{\partial x} \approx \frac{\partial u_i}{\partial z} \tag{40}$$

$i = 0$ and 90 deg. The coefficient $\bar{G}$ is done by

$$\bar{G} = 3G/t_{90} \tag{41}$$

The generalized shear modulus of the elementary cell

$$G = G_{xz}^{90}\Big/\left\{1 - 3\left(G_{xz}^{90}\big/G_{xz}^0\right)[f(t_{90})/f'(t_{90})]\right\} \tag{42}$$

Two different analytical functions of the variation function have been considered:

1) A complete parabolic model,[7–9]

$$f(z) = z^2 - 2(t_0+t_{90})z + \tfrac{2}{3}t_0^2 + 2t_0t_{90} + t_{90}^2 \tag{43}$$

2) A progressive shear model,[8,9]

$$f(z) = \frac{\sin(t_0/t_{90})\eta_t}{(t_0/t_{90})\eta_t} - \cosh\,\eta_t\left(1+\frac{t_0}{t_{90}}-\frac{z}{t_{90}}\right) \tag{44}$$

Characterized by the shear-transfer parameter

$$\eta_t = \left(E_0\big/G_{xz}^0\right)(1/\bar{l}_0) \tag{45}$$

2. Generalized Hashin's Model (Variational Model)

In the original model uniform axial-stress distribution across the layer thickness is assumed in 0- and 90-deg layers.[10] This assumption gives linear distributions for shear stresses and parabolic for z-axis normal stress. Expressions for x-axis stress components are the following:

$$\sigma_x^{90} = \sigma_{x0}^{90}[1-\psi(\bar{x})], \qquad \sigma_x^0 = \sigma_{x0}^0 + \sigma_{x0}^{90}(1/\alpha)\psi(\bar{x}) \tag{46}$$

where σ_{x0}^{90} is the stress in 90-deg layer and σ_{x0}^0 is the stress in the 0-deg layer before cracking. By using this assumption, final expression for complementary energy will be in the form of

$$V = V_0 + \frac{\left(\sigma_{x0}^{90}\right)^2 t_{90}^2}{2}\int_{-\bar{l}_0}^{\bar{l}_0}\mathrm{d}\bar{x}\left\{C_{00}\psi(\bar{x})^2 + C_{02}\psi(\bar{x})\psi''(\bar{x}) + C_{22}[\psi''(\bar{x})]^2 + C_{11}[\psi'(\bar{x})]^2\right\} \tag{47}$$

where

$$C_{00} = 1/E_{90} + (1/E_0)(1/\alpha)$$

$$C_{02} = (\nu_{23}/E_{90})\left(\alpha + \tfrac{2}{3}\right) - (\nu_{13}/3E_0)\alpha$$

$$C_{11} = 1/3G_{23} + (1/3G_{13})\alpha$$

$$C_{22} = [(\alpha+1)/60E_{90}](3\alpha^2 + 12\alpha + 8) \tag{48}$$

Minimization of the complementary energy [Eq. 47] with respect to $\psi(x)$ leads to fourth-order differential equation with constant coefficients for this function. Roots of the corresponding characteristic equation are as follows:
$k = \pm(\delta \pm i\beta)$, where

$$\delta = q^{\frac{1}{4}}\cos(\theta/2), \qquad \beta = q^{\frac{1}{4}}\sin(\theta/2)$$

$$\tan\theta = \sqrt{4q/p^2 - 1} \tag{49}$$

provided $4q > p^2$ and

$$p = (C_{02} - C_{11})/C_{22}, \qquad q = C_{00}/C_{22} \tag{50}$$

The final expression for $\psi(x)$ because of symmetry with respect to $x = 0$ is as follows:

$$\psi = A_1\cosh(\delta\bar{x})\cos(\beta\bar{x}) + A_2\sinh(\delta\bar{x})\sin(\beta\bar{x}) \tag{51}$$

Coefficients A_i can be obtained from zero axial- and shear-stress boundary conditions on the crack surface. Perturbation function $R(\bar{l}_0)$ can now be found as follows:

$$R(\bar{l}_0) = \int_{-\bar{l}_0}^{+\bar{l}_0}\psi(\bar{x})\,\mathrm{d}\bar{x} \tag{52}$$

By performing integration, we obtain

$$R(\bar{l}_0) = \frac{4\delta\beta}{\delta^2+\beta^2}\,\frac{\cosh(2\delta\bar{l}_0) - \cos(2\beta\bar{l}_0)}{\beta\,\sinh(2\delta\bar{l}_0) + \delta\,\sin(2\beta\bar{l}_0)} \tag{53}$$

III. Results and Discussion

A computer code based on the preceding equations was written to compute the stiffness loss of cross-ply laminates caused by the transverse ply cracking tacking into account the hygrothermal effect on the elastic properties.

A. Verification of the Modified Models

Before analyzing the reduced longitudinal Young's modulus of cross-ply laminates vs cracks density with the taking into account the hygrothermal effect on the material properties of the laminate, we check the results obtained by the used modified models with the existing experimental data.

Material properties of typical graphite/epoxy and glass/epoxy composite systems used in the present analysis are given in Table 1 (Ref. 29). The effect of transverse cracks on the stiffness reduction of the $[0/90_n]_S$ cross-ply laminate family is evaluated by a modified shear-lag models and Hashin's model. Figures 2–4 show the

Table 1 Material properties of composite systems used in calculations

Property	AS4-3502[29]	Glass/epoxy[1]
E_L, GPa	144.8	41.7
E_T, GPa	9.58	13.0
G_{LT}, GPa	4.79	3.4
$G_{TT'}$, GPa	4.2	4.58
ν_{LT}	0.31	0.3
ν_{TL}	0.4	0.42
h_0, mm	0.127	0.203

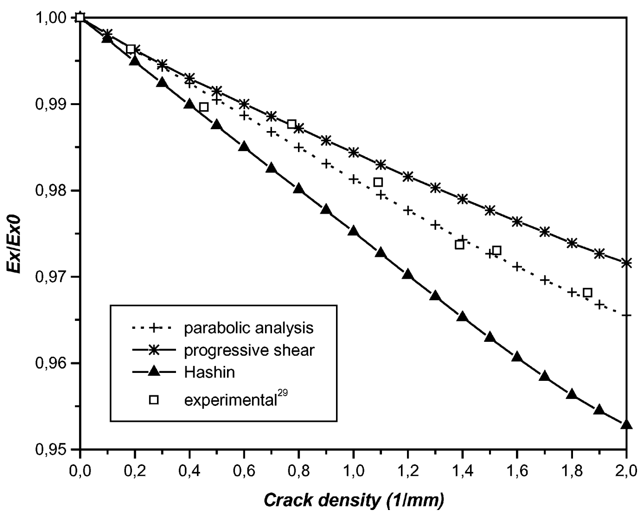

Fig. 2 Stiffness reduction caused by transverse cracks in a [0/90]$_S$ AS/3502 laminate.

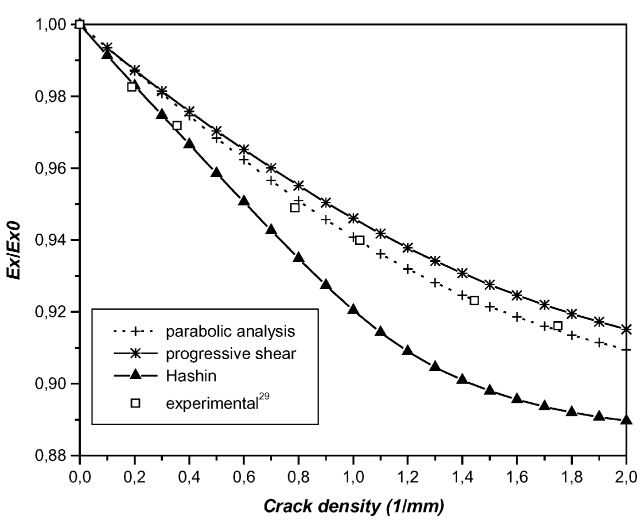

Fig. 3 Stiffness reduction caused by transverse cracks in a [0/90$_2$]$_S$ AS/3502 laminate.

comparison of the present predictions of stiffness reduction caused by transverse cracks with experimental data for the AS4-3502 graphite/epoxy cross-ply laminate family. It is shown that when cracking in transverse layer occurs stiffness of the laminate changes. The best fit with experimental data gives the shear-lag model, which assumes a complete parabolic displacement distribution. Hashin's model predicts much larger changes than in experiment.

Figure 5 presents the phenomenon that stiffness reduction is aggravated with the increment of 90-deg thickness. In fact, the stiffness reduction becomes more marked with increasing 90-deg layer thickness. This is explained by the fact that by increasing the 90-deg layer thickness, more loads are carried by the 90-deg layer and a larger crack-opening displacement of a transverse crack results for a given applied load.

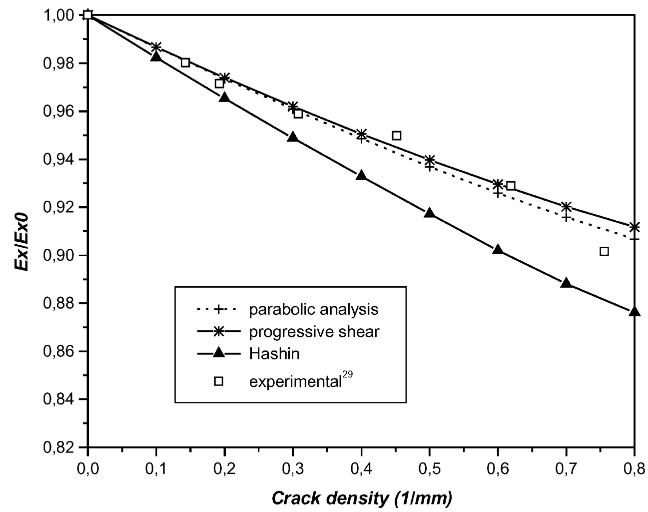

Fig. 4 Stiffness reduction caused by transverse cracks in a [0/90$_3$]$_S$ AS/3502 laminate.

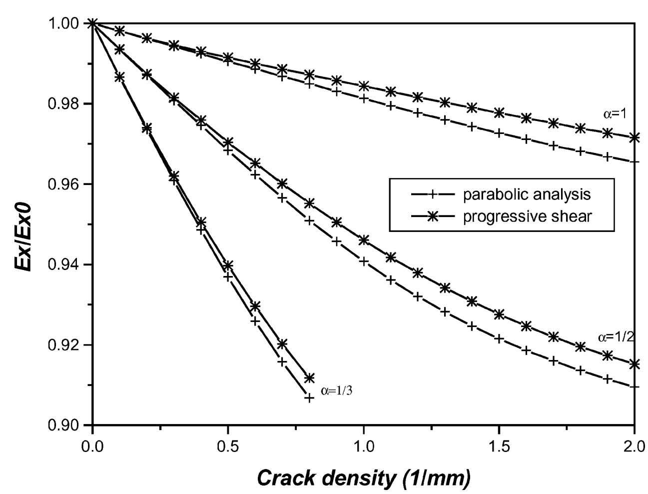

Fig. 5 Evaluation of the longitudinal Young's modulus of AS4/3502 laminates as a function of the crack density for three stacking sequences: [0/90]$_S$ ($\alpha = 1$), [0/90$_2$]$_S$ ($\alpha = 1/2$), and [0/90$_3$]$_S$ ($\alpha = 1/3$).

Figure 6 shows the stiffness reduction of a [0/90$_3$]$_S$ E-glass/epoxy cross-ply laminate. In this case the best fit with experimental data gives Hashin's model. The discrepancy between the results predicted by using the two shear-lag models and the experimental data are greater than for the graphite/epoxy cross-ply laminate family of Figs. 2–4. However, the general character of the predicted curve suggests similarity with experimental data. Some difference between the analytical model and experiment is expected in any case because the damage mode in the present analysis is restricted to uniformly distribute straight transverse cracks. In practice, because of the random nature of the transverse cracking behavior, the uniform distribution of straight transverse cracks does not occur exactly in thick cracking layers.

B. Influence of Hygrothermal Conditions on the Reduced Young's Modulus

The study here has focused on the stiffness reduction caused by transverse ply cracking in simple cross-ply laminate when the latter is initially exposed to the hygrothermal aging. For that, several numerical examples were presented. Graphite/epoxy composite material was selected in the present examples. However, the analysis is equally applicable to other types of composite material. For these examples the thickness of each ply is 0.125 mm, and the material properties adopted are as follows[16–18]: $E_f = 230.0$ GPa, $G_f = 9.0$ GPa, $\nu_f = 0.203$, $\nu_m = 0.34$, and $E_m = (3.51 - 0.003T - 0.142C)$ GPa,

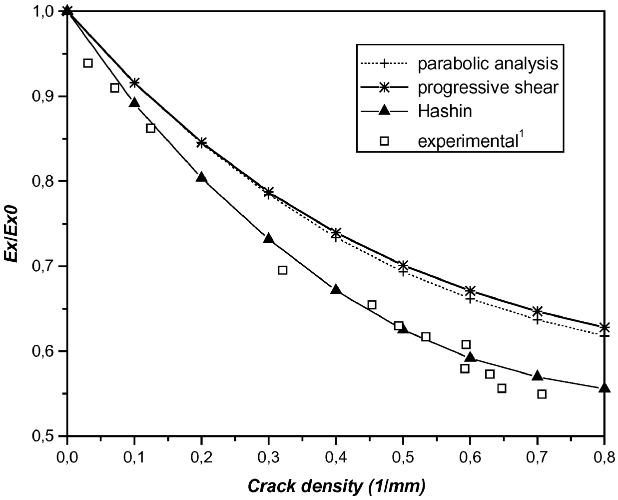

Fig. 6 Stiffness reduction caused by transverse cracks in a $[0/90_3]_S$ E-glass/epoxy laminate.

in which $T = T_0 + \Delta T$ and $T_0 = 25°C$ (room temperature) and $C = C_0 + \Delta C$ and $C_0 = 0$ wt% H_2O. Three sets of environmental conditions are considered, referred to as 1, 2, and 3. For environmental case 1, $T = 25°C$, so that both ΔT and ΔC are zero. For environmental case 2, $\Delta T = 50°C$ and $\Delta C = 0.5\%$, and for environmental case 3, $\Delta T = 100°C$ and $\Delta C = 1\%$. Also, three values of the fiber volume fraction $V_f (= 0.5, 0.6, \text{and } 0.7)$ are considered. The environmental case 1 will be regarded as the reference case.

1. Prediction of Relative Elastic Moduli

We calculate here the relative loss of stiffness in laminate, which is already subjected to the hygrothermal aging of type 1, 2, or 3. The loss of stiffness in the laminate as a result of crack density is evaluated compared to the initial stiffness of the uncracked laminate with the same environmental case 1, 2, or 3. We note that this initial stiffness of the uncracked laminate is a function of temperature and moisture. Consequently, Eq. (34) becomes

$$E_{x(i)}/E_{x0(i)} = 1\Big/\left[1 + a_{(i)}\bar{\rho}R_{(i)}(\bar{l}_0)\right] \tag{54}$$

The index (i) represents the considered case of the environmental conditions (case 1, 2, or 3). The results obtained are reported in Figs. 7 and 8 using both modified models: the complete parabolic shear-lag model[7–9] and the progressive shear-lag model.[8,9] The modulus reduction depends in addition to the crack density on the moisture and temperature. In fact, the longitudinal Young's modulus is reduced with decreases in moisture and temperature especially when the crack density becomes higher.

Figures 9 and 10 show the effect of fiber volume fractions $V_f (= 0.5, 0.6, \text{and } 0.7)$ on the variation of longitudinal Young's modulus with crack density and under the environmental conditions of case 1. The calculation is carried out by using the two considered models. It can be seen that longitudinal Young's modulus is reduced with increases in fiber volume fraction.

2. Analysis of Total Stiffness Reduction

In this section, the variation of longitudinal Young's modulus as a function of crack density and environmental effect is investigated by using the two considered models. The total reduction of the longitudinal Young's modulus is determined compared to the longitudinal Young's modulus of the uncracked laminate when the latter is exposed initially to the environmental conditions of case 1 (the reference case). Consequently, this total reduction of stiffness takes into account the reduction caused by the crack density and to the variation of moisture and temperature. Equation (34) becomes

$$\frac{E_{x(i)}}{E_{x0(1)}} = \frac{\left[\alpha E_{0(i)} + E_{90(i)}\right]}{\left[1 + a_{(i)}\bar{\rho}R_{(i)}(\bar{l}_0)\right]\left[\alpha E_{0(1)} + E_{90(1)}\right]} \tag{55}$$

The variation of longitudinal Young's modulus is plotted in Figs. 11 and 12 as a function of crack density for three cases of environmental

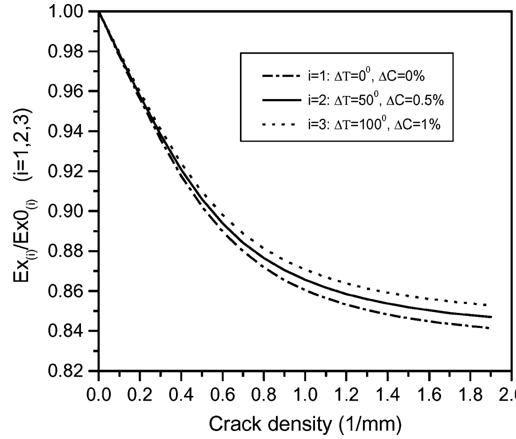

Fig. 7 Relative modulus reduction in a $[0/90_3]_S$ graphite/epoxy laminate as a function of crack density. The calculation is carried out by using the complete parabolic model ($V_f = 0.6$).

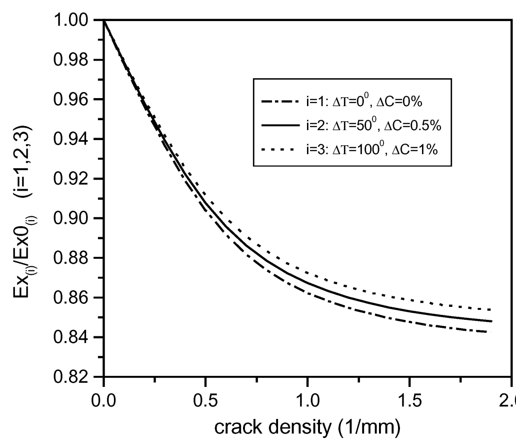

Fig. 8 Relative modulus reduction in a $[0/90_3]_S$ graphite/epoxy laminate as a function of crack density. The calculation is carried out by using the progressive shear model ($V_f = 0.6$).

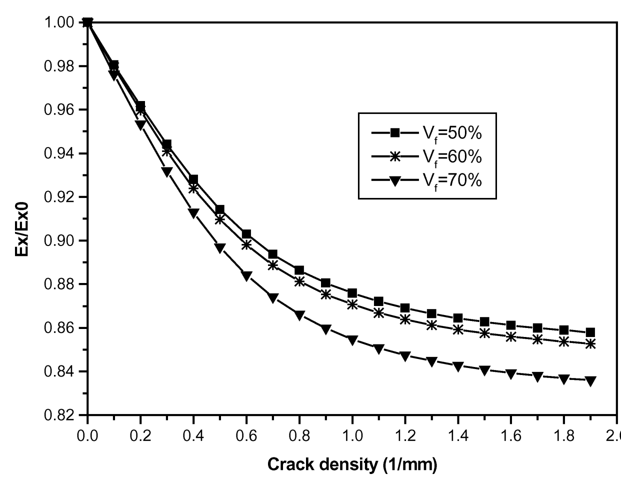

Fig. 9 Effect of fiber volume fraction on relative modulus reduction in a $[0/90_3]_S$ graphite/epoxy laminate as a function of crack density. The calculation is carried out by using the complete parabolic model ($\Delta T = 0°C$, $\Delta C = 0\%$).

conditions 1, 2, and 3. It can be observed that for a zero crack density there is a reduction of longitudinal Young's modulus, which is related completely to the effects of hygrothermal conditions. With increases in crack density, the sensitivity of the hygrothermal effects on the modulus reduction becomes weaker. In contrast with the relative reduction of longitudinal Young's modulus, the total reduction of longitudinal Young's modulus increases with moisture content and temperature especially at lower crack density.

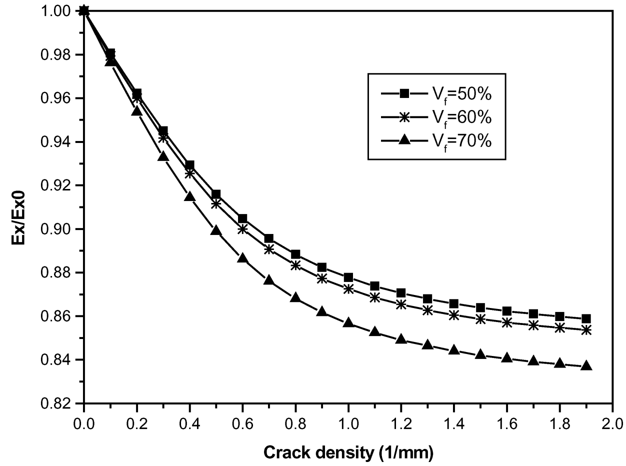

Fig. 10 Effect of fiber volume fraction on relative modulus reduction in a $[0/90_3]_S$ graphite/epoxy laminate as a function of crack density. The calculation is carried out by using the progressive shear model ($\Delta T = 0°C$, $\Delta C = 0\%$).

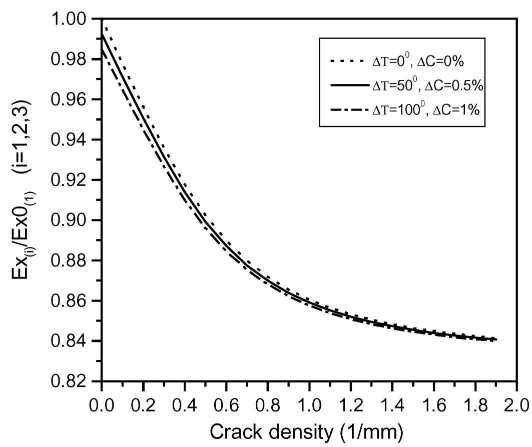

Fig. 11 Total modulus reduction in a $[0/90_3]_S$ graphite/epoxy laminates ($V_f = 0.6$) as a function of the crack density by using the complete parabolic model.

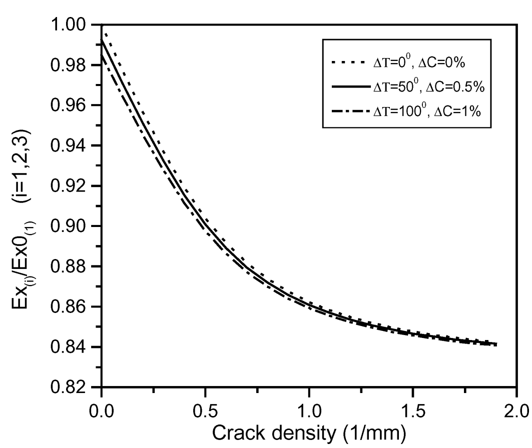

Fig. 12 Total modulus reduction in a $[0/90_3]_S$ graphite/epoxy laminates ($V_f = 0.6$) as a function of the crack density by using the progressive shear model.

IV. Conclusions

A modified shear-lag analysis by introducing the stress perturbation function has been used to evaluate the effect of transverse cracks on the stiffness reduction in a family of cross-ply laminates. Predictions of the reduced longitudinal Young's modulus due to transverse cracks are compared with existing experimental data. In the second part of this study, the effects of temperature and moisture on the reduction of the longitudinal Young's modulus in cross-ply laminates containing transverse cracking were investigated. On the basis of the present results the following conclusion can be drawn:

1) Transverse cracks reduce the effective stiffness in composite laminates.

2) The stiffness reduction caused by transverse cracks is profoundly influenced by the laminate configuration.

3) The decreases in moisture and temperature reduce the relative stiffness of laminate, especially when the crack density becomes higher.

4) The total reduction of longitudinal Young's modulus increases with moisture content and temperature especially at lower crack density.

5) The increases in fiber volume fraction reduce the effective stiffness of laminate.

References

[1] Highsmith, A. L., and Reifsnider, K. L., "Stiffness Reduction Mechanism in Composite Laminates," *Damage in Composite Materials*, ASTM STP 775, edited by K. L. Reifsnider, American Society for Testing and Materials, 1982, pp. 103–117.

[2] Flaggs, D. L., "Prediction of Tensile Failure in Composite Laminates," *Journal of Composite Materials*, Vol. 19, No. 1, 1985, pp. 103–116.

[3] Laws, N., and Dvorak, G. J., "Progressive Transverse Cracking in Composite Laminates," *Journal of Composite Materials*, Vol. 22, 1988, pp. 900–916.

[4] Lim, S. G., and Hong, C. S., "Prediction of Transverse Cracking and Stiffness Reduction in Cross-Ply Laminated Composites," *Journal of Composite Materials*, Vol. 23, July 1989, pp. 695–713.

[5] Lim, S. G., and Hong, C. S., "Effect of Transverse Cracks on the Thermomechanical Properties of Cross-Ply Laminated Composites," *Composites Science and Technology*, Vol. 34, No. 2, 1989, pp. 145–162.

[6] Lee, J. W., and Daniel, I. M., "Progressive Transverse Cracking of Cross-Ply Composite Laminates," *Journal of Composite Materials*, Vol. 24, No. 11, 1990, pp. 1225–1243.

[7] Berthelot, J. M., Leblond, P., El Mahi, A., and Le Corre, J. F., "Transverse Cracking of Cross-Ply Laminates. Part 1: Analysis," *Composites Part A*, Vol. 27, No. 10, 1996, pp. 989–1001.

[8] Berthelot, J. M., "Analysis of the Transverse Cracking of Cross-Laminates: A Generalized Approach," *Journal of Composite Materials*, Vol. 31, No. 18, 1997, pp. 1780–1805.

[9] Berthelot, J. M., and Le Corre, J. F., "Modelling the Transverse Cracking in Cross-Ply Laminates: Application to Fatigue," *Composites Engineering Part B*, Vol. 30, No. 6, 1999, pp. 569–577.

[10] Hashin, Z., "Analysis of Cracked Laminates: a Variational Approach," *Mechanics of Material*, Vol. 4, No. 2, 1985, pp. 121–136.

[11] Varna, J., and Berglund, L., "Multiple Transverse Cracking and Stiffness Reduction in Cross-Ply Laminates," *Journal of Composites Technology and Research*, Vol. 13, No. 2, 1991, pp. 97–106.

[12] Nairn, J. A., "The Strain Energy Release Rate of Composite Microcracking: A Variational Approach," *Journal of Composite Materials*, Vol. 23, No. 11, 1989, pp. 1106–1129.

[13] Dharani, L. R., and Tang, H., "Micromechanics Characterization of Sublaminate Damage," *International Journal of Fracture*, Vol. 46, No. 2, 1990, pp. 123–140.

[14] Selvarathinam, A. S., and Weitsman, Y. J., "Transverse Cracking and Delamination in Cross-Ply gr/ep Composites Under Dry, Saturated and Immersed Fatigue," *International Journal of Fracture*, Vol. 91, No. 2, 1998, pp. 103–116.

[15] Shen, C. H., and Springer, G. S., "Environmental Effects in the Elastic Moduli of Composite Material," *Environmental Effects on Composite Materials*, edited by G. S. Springer, Technomic, Westport, CT, 1981, pp. 94–108.

[16] Adams, D. F., and Miller, A. K., "Hygrothermal Microstresses in a Unidirectional Composite Exhibiting Inelastic Materials Behaviour," *Journal of Composite Materials*, Vol. 11, 1977, pp. 285–299.

[17] Bowles, D. E., and Tompkins, S. S., "Prediction of Coefficients of Thermal Expansion for Unidirectional Composites," *Journal of Composite Materials*, Vol. 23, 1989, pp. 370–381.

[18] Shen, H. S., "Hygrothermal Effects on the Postbuckling of Composite Laminated Cylindrical Shells," *Composites Science and Technology*, Vol. 60, No. 8, 2000, pp.1227–1240.

[19] Megueni, A., Tounsi, A., Bouiadjra, B. B., and Serier, B., "The Effect of a Bonded Hygrothermal Aged Composite Patch on the Stress Intensity Factor for Repairing Cracked Metallic Structures," *Composite Structures*, Vol. 62, No. 2, 2003, pp. 171–176.

[20] Tounsi, A., and Adda-Bedia, E. A., "Simplified Method for Prediction of Transient Hygroscopic Stresses in Polymer Matrix Composites with Symmetric Environmental Conditions," *Journal of Applied Composite Materials*, Vol. 10, No. 1, 2003, pp. 1–18.

[21]Tounsi, A., and Adda Bedia, E. A., "Some Observations on the Evolution of Transversal Hygroscopic Stresses in Laminated Composites Plates: Effect of Anisotropy," *Composite Structures*, Vol. 59, No. 4, 2003, pp. 445–454.

[22]Adda-Bedia, E. A., Tounsi, A., and Sereir, Z., "A Quantitative Study on the Influence of Anisotropy on the Hygrothermal Behaviour of the Laminated Composite Plates," *Eighth International Conference on Composite Engineering ICCE8*, 2001.

[23]Benkeddad, A., Grediac, M., and Vautrin, A., "Computation of Transient Hygroscopic Stresses in Laminated Composite Plates," *Composites Science and Technology*, Vol. 56, No. 7, 1996, pp. 869–876.

[24]Benkeddad, A., Grediac, M., and Vautrin, A., "On the Transient Hygroscopic Stresses in Laminated Composite Plates," *Composite Structures*, Vol. 30, No. 2, 1995, pp. 201–205.

[25]Hahn, H. T., and Kim, R. Y., "Swelling of Composite Laminates," *Advanced Composite Materials—Environmental Effects*, ASTM STP 658, edited by J. R. Vinson, American Society for Testing and Materials, 1978, pp. 98–120.

[26]Kim, H. W., Grayson, M. A., and Nairn, J. A., "The Effects of Hygrothermal Aging on the Microcracking Properties of Some Carbon Fiber/Polyimide Laminates," *Advanced Composite Letters*, Vol. 4, No. 5, 1995, pp. 185–188.

[27]Tsai, S. W., and Hahn, H. T., *Introduction to Composite Materials*, Technomic, Westport, CT, 1980.

[28]Joffe, R., Krasnikovs, A., and Varna, J., "COD-Based Simulation of Transverse Cracking and Stiffness Reduction in $[S/90_n]_S$ Laminates," *Composites Science and Technology*, Vol. 61, No. 5, 2001, pp. 637–656.

[29]Groves, S. E., Harris, C. E., Highsmith, A. L., Allen, D. H., and Norvell, R. G., "An Experimental and Analytical Treatment of Matrix Cracking in Cross-Ply Laminates," *Experimental Mechanics*, Vol. 27, No. 1, 1987, pp. 73–79.

K. Shivakumar
Associate Editor